 DOI: 10.1002/eji.201444795 Eur. J. Immunol. 2015. 45: 818–828

European Journal of Immunology

A20 expression in dendritic cells protects mice from LPS-induced mortality

Nguyen Thi Xuan[*1], Xu Wang*[*1], Gopala Nishanth[1], Ari Waisman[2], Katrin Borucki[3], Berend Isermann[3], Michael Naumann[4], Martina Deckert[5] and Dirk Schlüter[1,6]*

[1] Institute of Medical Microbiology and Hospital Hygiene, Otto-von-Guericke University Magdeburg, Magdeburg, Germany
[2] Institute for Molecular Medicine, University of Mainz, Mainz, Germany
[3] Institute of Clinical Chemistry and Pathobiochemistry, Otto-von-Guericke University Magdeburg, Magdeburg, Germany
[4] Institute of Experimental Internal Medicine, Otto-von-Guericke University Magdeburg, Magdeburg, Germany
[5] Department of Neuropathology, University of Cologne, Cologne, Germany
[6] Helmholtz Centre for Infection Research, Braunschweig, Germany

DCs contribute to immune homeostasis under physiological conditions and regulate the immune activation during infection. The deubiquitinase A20 inhibits the activation of NF-κB-dependent immune reactions, and prevents the hyperactivation of DCs under steady-state conditions. However, the role of DC-specific A20 under pathological conditions is unknown. Here, we demonstrate that upon injection of low-dose LPS, mice with DC-specific A20 deletion (CD11c-Cre A20$^{fl/fl}$) died within 6 h, whereas A20$^{fl/fl}$ controls survived. LPS-induced mortality in CD11c-Cre A20$^{fl/fl}$ mice was characterized by increased serum levels of IL-2, IL-10, IL-12, IFN-γ, and TNF. Upon LPS stimulation, the activation of NF-κB and ERK-NFATc3 pathways were enhanced in A20-deficient DCs, resulting in an increased production of IL-2, IL-12, and TNF both in vitro and in vivo. Targeted inhibition of ERK in A20-deficient DCs abolished the increased production of IL-2. A20-deficient DCs failed to induce LPS tolerance, which was independent of T cells and the intestinal flora, since T-cell depletion and decolonization of CD11c-Cre A20$^{fl/fl}$ mice could not prevent death of LPS-challenged CD11c-Cre A20$^{fl/fl}$ mice. In conclusion, these findings show that DC-specific A20 preserves immune homeostasis in steady-state conditions and is also required for LPS tolerance.

Keywords: A20 · Autoimmunity · DC · LPS tolerance · Mice

Additional supporting information may be found in the online version of this article at the publisher's web-site

Introduction

DCs are specialized sentinel cells that bridge innate and adaptive immune responses. During infection and immunization, DCs detect inflammation, or pathogens via pattern recognition receptors (PPRs), such as TLRs, and present pathogen-derived antigens to antigen-specific T cells [1]. PPRs-activated DCs also upregulate the expression of MHC molecules, costimulatory molecules, and

Correspondence: Prof. Dirk Schlüter
e-mail: dirk.schlueter@med.ovgu.de

*These authors contributed equally to this work.

cytokines, thereby leading to the recruitment and activation of various types of immune cells [2, 3].

Among the PPRs, TLRs are the best characterized subgroup. So far, ten human and 12 murine TLRs have been characterized, and each of them is activated by a distinct set of pathogen-associated molecular patterns (PAMPs) [4, 5]. TLRs are categorized based on their specific adaptor molecules. TLR3 signals via the TIR-domain-containing adapter-inducing IFN-β (TRIF) adaptor, while all other TLRs signal via the MyD88 adaptor [6]. TLR4 is the only TLR able to activate both TRIF and MyD88 adaptors.

LPS binds specifically to TLR4 and activates two distinct signaling pathways: a MyD88-dependent and MyD88-independent pathway [7, 8]. Engagement of TLR4 on the plasma membrane by LPS results in the recruitment of MyD88 and a large multiprotein complex at the cytoplasmic face of the plasma membrane, which leads to activation of NF-κB and MAPKs and the subsequent production of proinflammatory cytokines and chemokines [7]. Then activated TLR4 translocates to an endosomal compartment triggering a MyD88-independent pathway. Internalized TLR4 recruits TRIF and TRIF-related adaptor molecule (TRAM), which activates interferon regulatory factor-3 (IRF3) leading to the production of type I IFNs [9–11]. In addition, MyD88-independent signaling also involves the activation of NF-κB.

NF-κB activation is negatively regulated by A20, a ubiquitin-modifying enzyme [12]. A20 inhibits activation of NF-κB by cleaving K63-linked polyubiquitin chains from multiple target molecules including receptor-interacting protein 1 (RIP1), TNF receptor associated factor 6 (TRAF6), and NF-kappa-B essential modulator (NEMO), and targets key intermediate NF-κB signaling molecules, including RIP1, for proteasomal degradation by adding K48-linked polyubiquitin chains [13–15]. The anti-inflammatory role of A20 is reflected by the phenotype of conventional A20-deficient mice, which spontaneously harbor activated and expanded myeloid cells resulting in multiorgan inflammation, cachexia, and, finally, death [16]. Consistently, selective ablation of A20 in DCs causes spontaneous DC activation, resulting in either autoantibody-mediated nephritis and arthritis or a lymphocyte-dependent colitis, spondylarthritis, and enthesitis, respectively [17, 18]. In addition, the premature lethality and cachexia of A20-deficient mice can be prevented by ablation of MyD88 [19], indicating that suppression of TRIF-dependent signaling by A20 plays a minor role, if any, in the spontaneous disease of mice lacking A20 in DCs. In agreement, A20 has been shown to inhibit LPS-induced MyD88-dependent TNF and IL-6 production in DCs [17, 19], suggesting that A20 is also involved in the regulation of TLR4-mediated signaling pathways in DCs. However, the molecular mechanisms as well as the precise in vivo role of A20 in LPS-stimulated DCs are unclear.

To address the role of A20 in TLR4-mediated DC activation, we treated A20-sufficient and -deficient DCs with LPS and observed that A20 restricted LPS-induced NF-κB and ERK-NFATc3 pathways in DCs. Exaggerated signaling in A20-deficient DCs resulted in increased production of proinflammatory cytokines. As a result, mice with DC-specific A20 deletion failed to tolerate LPS and died within 6 h after challenge with low doses of LPS.

Results

Spontaneous multiorgan inflammation in CD11c-Cre A20$^{fl/fl}$ mice

To explore the role of A20 derived from DCs, we generated CD11c-Cre A20$^{fl/fl}$ mice, which specifically lacked A20 in DCs (Fig. 1A). In contrast to the postnatal lethality of A20-deficient mice, CD11c-Cre A20$^{fl/fl}$ mice survived although they developed spontaneous multiorgan inflammation (Supporting Information Fig. 1). In contrast to previous reports [17, 18], inflammation of CD11c-Cre A20$^{fl/fl}$ mice was particularly prominent in the liver (Supporting Information Fig. 1). Consistently, serum levels of proinflammatory cytokines IL-2, TNF, and IFN-γ were upregulated in CD11c-Cre A20$^{fl/fl}$ mice (Fig. 1B). Fms-related tyrosine kinase 3 ligand (FLT3L), a cytokine that strongly increases numbers of mature DCs [20], was also significantly increased in serum of CD11c-Cre A20$^{fl/fl}$ mice (Fig. 1C). In agreement, numbers of CD11c$^+$, CD11c$^+$ CD11b$^+$ CD8α$^-$, and CD11c$^+$ DC-SIGN$^+$ cells were significantly increased in both spleens and livers of CD11c-Cre A20$^{fl/fl}$ mice as compared with controls (Fig. 1D). In addition, expression of MHC class II, CD86, and CD40 was strongly increased on DCs in inflamed organs of CD11c-Cre A20$^{fl/fl}$ mice (Fig. 1E), showing that A20 prevents spontaneous activation of DCs in parenchymatous organs.

CD11c-Cre A20$^{fl/fl}$ mice succumb to low-dose LPS

To study the role of A20 in DCs under pathophysiological conditions, we analyzed the influence of systemic low-dose LPS stimulation on CD11c-Cre A20$^{fl/fl}$ *mice*. CD11c-Cre A20$^{fl/fl}$ *mice* died within 6 h after injection of LPS, whereas all A20$^{fl/fl}$ *mice* survived (Fig. 2A). After LPS challenge, serum levels of proinflammatory IL-2, IL-12, TNF, and IFN-γ, as well as anti-inflammatory IL-10 were all markedly elevated in CD11c-Cre A20$^{fl/fl}$ mice as compared with A20$^{fl/fl}$ mice (Fig. 2B), indicating that CD11c-Cre A20$^{fl/fl}$ mice died from unfettered cytokine response to LPS. DCs have been shown to be a major source of cytokines; therefore, we studied cytokine production of DCs before and after LPS challenge. After LPS stimulation, numbers of IL-2-, IL-12-, and TNF-producing CD11c$^+$ DCs were elevated, although not all significantly, in spleens of CD11c-Cre A20$^{fl/fl}$ mice and all of these DC populations were significantly increased in livers of CD11c-Cre A20$^{fl/fl}$ mice as compared with control mice (Fig. 2C and Supporting Information Fig. 2). In addition, upon LPS stimulation, A20-deficient bone marrow-derived DCs (BMDCs) produced significantly more IL-2, IL-12, and TNF than A20-sufficient BMDCs (Fig. 2D). Taken together, these results show that the increased DC number and enhanced cytokine production of A20-deficient

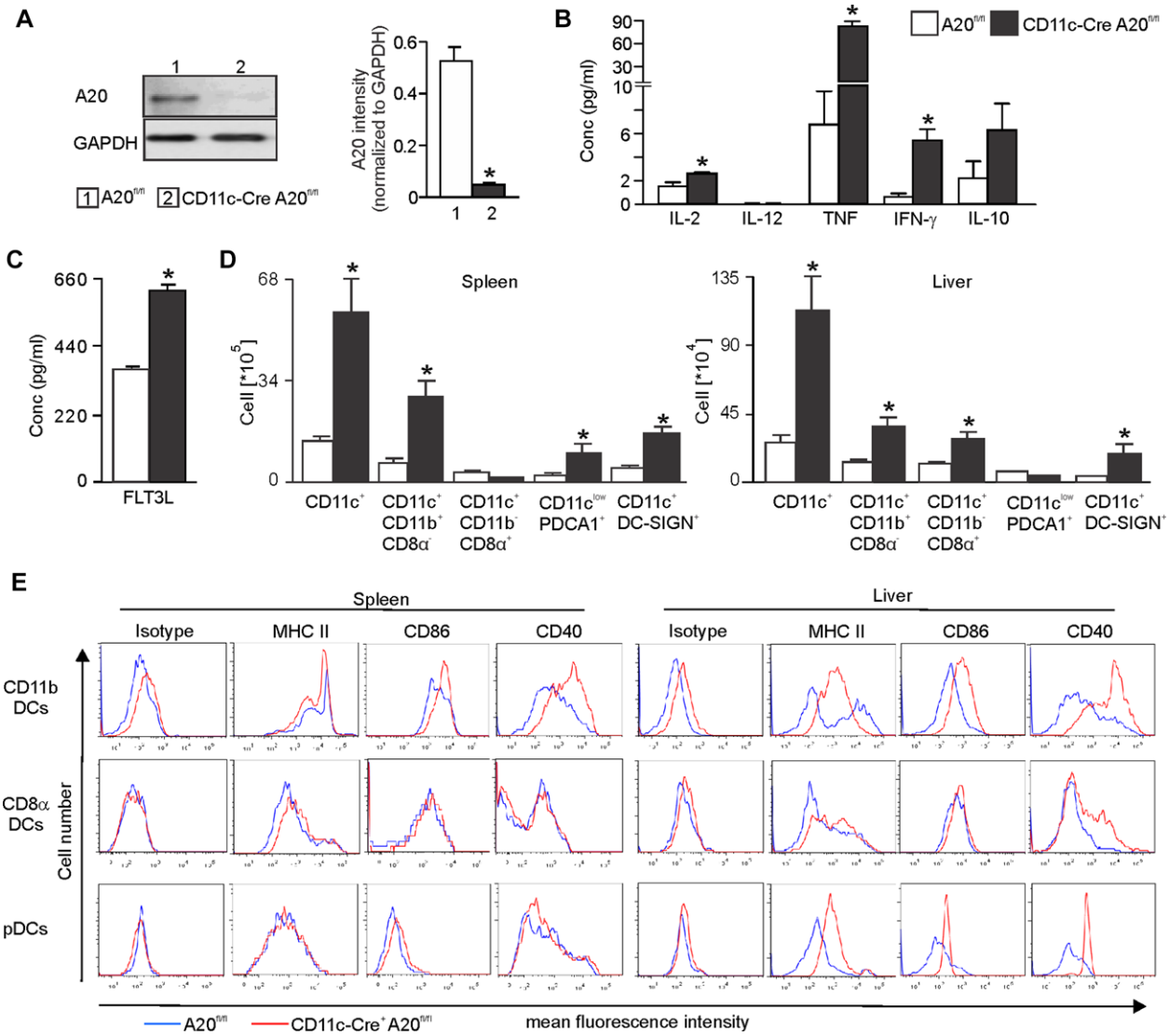

Figure 1. CD11c-Cre A20$^{fl/fl}$ mice develop spontaneous multiorgan inflammation. BMDCs were isolated from CD11c-Cre A20$^{fl/fl}$ and A20$^{fl/fl}$ control mice. (A) (Left panel) Western blot (WB) analysis of A20 expression, and (right panel) relative quantification of A20. (B) Serum levels of IL-2, IL-12, TNF, IFN-γ, and IL-10 were measured by cytometric bead arrays. (C) Serum levels of FLT3L were measured by flow cytometry. (D) Numbers of CD11c$^+$, CD11c$^+$ CD11b$^+$ CD8α$^-$, CD11c$^+$ CD11b$^-$ CD8α$^+$, CD11c^{low} PDCA1$^+$, and CD11c$^+$ DC-SIGN$^+$ cells were determined by flow cytometry. (E) The mean fluorescence intensity of MHC class II, CD86, and CD40 of splenic and hepatic CD11b DCs, CD8α DCs, and pDCs was analyzed by flow cytometry. (A–D) Data are shown as mean + SEM of 5–8 mice per experimental group and (A–E) are representative of (A) six or (B–E) three independent experiments. *$p < 0.05$; *t*-test.

DCs jointly contribute to the significantly increased cytokine production in CD11c-Cre A20$^{fl/fl}$ mice.

A20 negatively regulates NF-κB, MAPK, and NFAT pathways in BMDCs

To understand how A20 suppressed cytokine production in DCs, we studied signaling pathways activated by LPS. In both genotypes, LPS-stimulation of BMDCs resulted in an activation of Iκ-Bα and ERK1/2, which was, however, stronger in A20-deficient BMDCs (Fig. 3A and B). Activation of transforming growth factor-β activated kinase-1 (TAK1) and MEK1, which mediate ERK activation upon MyD88 stimulation, were also increased in A20-deficient BMDCs (Fig. 3A and B). In addition to BMDCs, MACS-isolated CD11c$^+$ DCs stimulated with LPS exhibited ERK activation, which was augmented in A20-deficient CD11c$^+$ cells (Supporting Information Fig. 3). Nuclear accumulation of activated NFATc3 was spontaneously enhanced in A20-deficient BMDCs and further upregulated by LPS-stimulation (Fig. 3C and D). Treatment of BMDCs with U0126, a selective MEK1 inhibitor, efficiently inhibited ERK1/2 activation (Fig. 3E). Treatment with U0126 induced a slightly increased apoptosis equally in both genotypes of LPS-stimulated BMDCs as compared with cells without

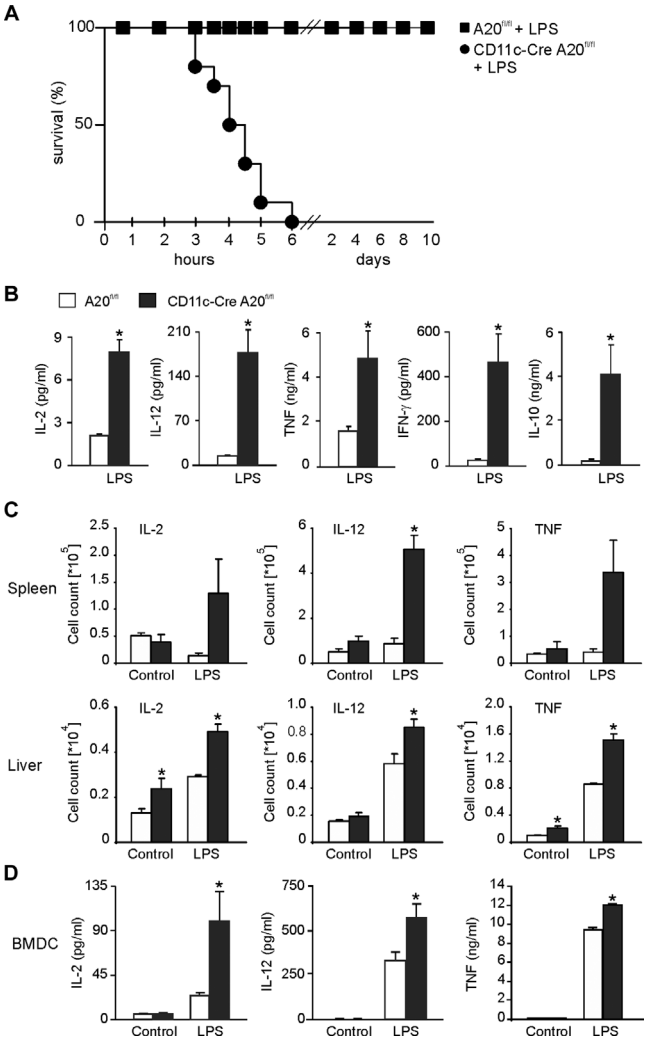

Figure 2. Increased sensitivity of CD11c-Cre A20$^{fl/fl}$ mice to a sublethal dose of LPS. (A) Survival of A20$^{fl/fl}$ and CD11c-Cre A20$^{fl/fl}$ mice after i.p. injection of LPS. Data are representative of three independent experiments, with 6–9 mice per experimental group. (B) Serum levels of IL-2, IL-12, TNF, IFN-γ, and IL-10 were measured by cytometric bead arrays 3 h after LPS injection. (C) Numbers of IL-2, IL-12, and TNF producing splenic (upper panel) and hepatic (lower panel) CD11c$^+$ DCs were determined by intracellular flow cytometry 3 h after LPS injection. (D) Concentration of IL-2, IL-12, and TNF produced by unstimulated and LPS-stimulated GM-CSF BMDCs were measured by cytometric bead arrays. (B–D) Data are shown as mean + SEM of 3–6 mice per experimental group and are from one experiment representative of three independent experiments. $^*p < 0.05$, *t*-test.

inhibitor treatment (Supporting Information Fig. 4A). ERK1/2 inhibition prior to LPS stimulation significantly reduced nuclear translocation and activation of NFATc3 in both A20-sufficient and A20-deficient BMDCs (Fig. 3F and G), abolished increased IL-2 production of A20-deficient BMDCs (Fig. 3H), but did not affect the A20-regulated TNF production, which is largely dependent on the canonical NF-κB activity (Supporting Information Fig. 4B).

Since NFATc3 activation in response to LPS is also regulated by CD14 and the calmodulin/calcineurin pathway [21], we performed additional experiments with the calmodulin inhibitor W7. Calmodulin inhibition strongly reduced IL-2 production (Fig. 3H). However, A20-deficient BMDCs still produced significantly more IL-2 than control BMDCs indicating that calmodulin-independent signaling pathways, which are regulated by A20, also mediate IL-2 production upon LPS stimulation. In good agreement, Western blot (WB) analysis showed that upon LPS + W7 treatment, nuclear accumulation of NFATc3 was still higher in A20-deficient BMDCs as compared with A20-sufficient BMDCs (Supporting Information Fig. 5). In contrast, ERK inhibition not only significantly reduced IL-2 production but also abolished the difference in IL-2 production between A20-deficient and A20-sufficient DCs (Fig. 3H).

Together these results show that, in response to LPS, A20 restricts cytokine production in BMDCs by inhibiting NF-κB, ERK, and NFATc3 pathways.

T cells are dispensable for low-dose LPS induced mortality of CD11c-Cre A20$^{fl/fl}$ mice

Since (i) IL-2 was significantly elevated in LPS-stimulated CD11c-Cre A20$^{fl/fl}$ mice, (ii) IL-2 regulates activation of T cells, and (iii) activated T cells are also potent producers of various cytokines, we investigated whether T cells contributed to the increased cytokine production and mortality of CD11c-Cre A20$^{fl/fl}$ mice in response to low-dose LPS. T cells were depleted in A20$^{fl/fl}$ and CD11c-Cre A20$^{fl/fl}$ mice with anti-CD4/CD8 antibodies (Fig. 4A). Upon LPS challenge, T-cell depletion did not prevent death of CD11c-Cre A20$^{fl/fl}$ mice, which died only a few hours later compared with rat IgG-treated CD11c-Cre A20$^{fl/fl}$ mice (Fig. 4B). In agreement with previous studies [22, 23], T-cell-depleted A20$^{fl/fl}$ control mice died from low-dose LPS challenge within 50 h (Fig. 4B) whereas all IgG-treated A20$^{fl/fl}$ mice survived (data not shown). In addition, only IL-12 production was significantly reduced in T-cell-depleted CD11c-Cre A20$^{fl/fl}$ mice as compared with IgG-treated CD11c-Cre A20$^{fl/fl}$ mice but levels of all other cytokines were still higher in T cell-depleted CD11c-Cre A20$^{fl/fl}$ mice as compared with A20$^{fl/fl}$ mice (Fig. 4C), demonstrating that DCs, but not T cells, are responsible for the elevated cytokine production and subsequent mortality of LPS-stimulated CD11c-Cre A20$^{fl/fl}$ mice. In addition, T-cell depletion only partially improved pathology of inflamed organs as indicated by the reduction of the liver enzymes alanine aminotransferase and aspartate aminotransferase in CD11c-Cre A20$^{fl/fl}$ mice (Supporting Information Fig. 6). However, T-cell depletion had no effect on the increased numbers of DC subsets and serum cytokine levels in CD11c-Cre A20$^{fl/fl}$ mice (Supporting Information Fig. 6).

Intestinal flora is dispensable for LPS-induced mortality in CD11c-Cre A20$^{fl/fl}$ mice

It has been reported that mice with DC-specific A20 deletion show perturbed bowel homeostasis and develop colitis spontaneously [17]. Therefore, exacerbation of colitis due to LPS challenge might

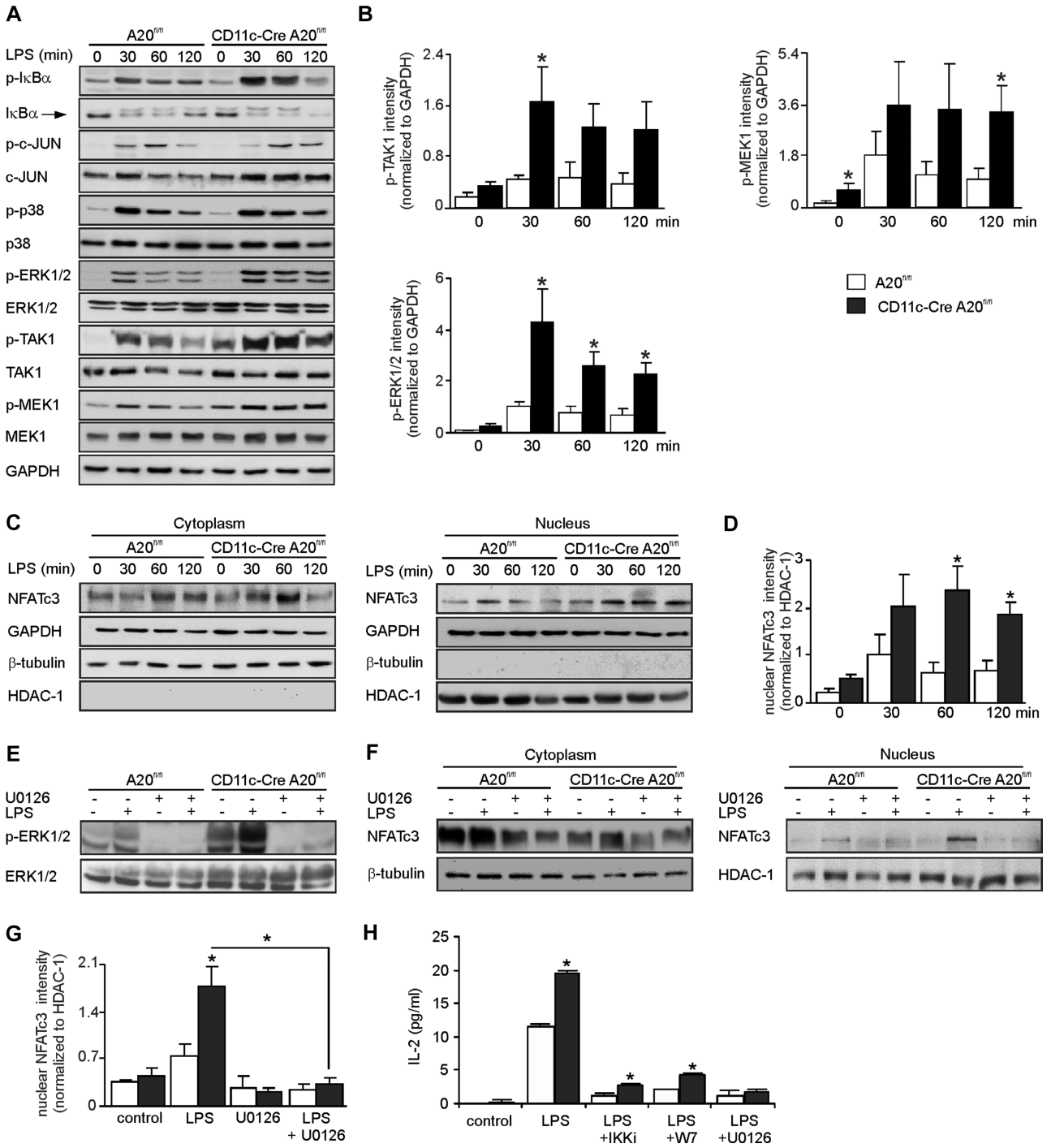

Figure 3. A20 negatively regulates ERK1/2-dependent cytokine production in BMDCs. (A) WB analysis of whole GM-CSF BMDC lysates stimulated with LPS for the indicated time points. (B) Quantification of p-TAK1, p-MEK1, and p-ERK after LPS stimulation for the indicated time points. $^*p < 0.05$, *t*-test. (C) WB analysis of cytoplasmic and nuclear extracts after LPS stimulation for the indicated time points. (D) Quantification of nuclear NFATc3 after LPS stimulation for the indicated time points. $^*p < 0.05$, *t*-test. (E and F) WB analysis of (E) whole cell lysates and (F) cytoplasmic and nuclear extracts unstimulated or stimulated with LPS and/or U0126. (G) Quantification of nuclear NFATc3 in GM-CSF BMDCs untreated or stimulated with LPS and/or U0126. $^*p < 0.05$, ANOVA test. (H) Concentrations of IL-2 produced by untreated and LPS stimulated GM-CSF BMDCs were measured by cytometric bead arrays. BMDCs were treated with IKK inhibitor, W7, or U0126 as indicated. $^*p < 0.05$ for CD11c-Cre A20$^{fl/fl}$ versus A20$^{fl/fl}$ BMDCs, *t*-test. (A–H) Data are shown as mean + SEM ($n = 3$) and are representative of at least three independent experiments.

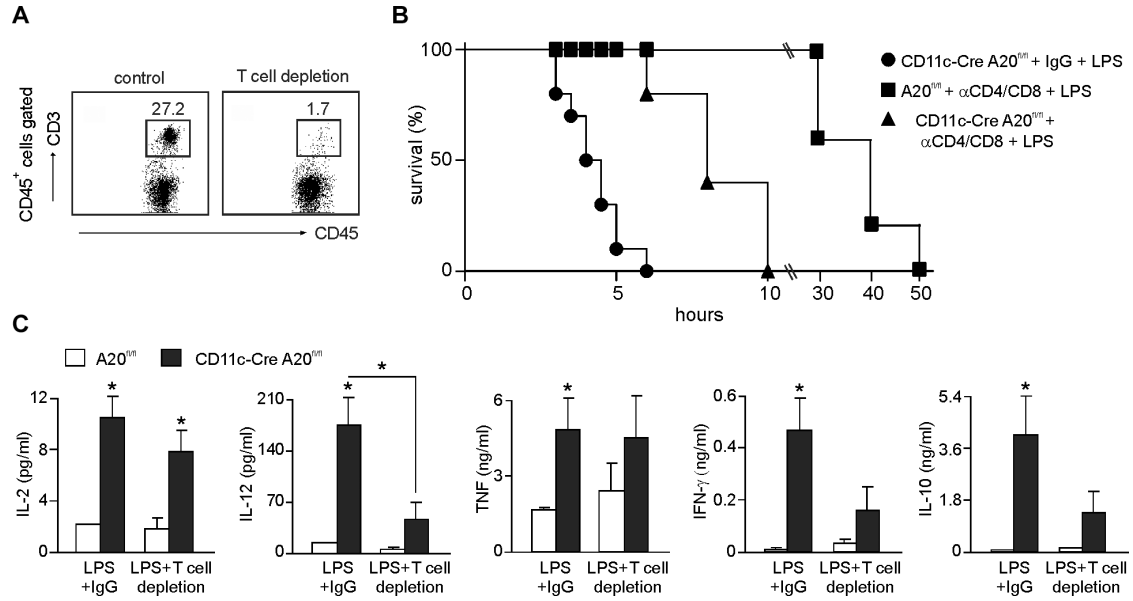

Figure 4. T-cell depletion does not rescue CD11c-Cre $A20^{fl/fl}$ mice from sublethal dose of LPS-mediated mortality. (A) Efficiency of T-cell depletion was measured by flow cytometry ($n = 3$ mice/group). (B) Survival of LPS-treated CD11c-Cre $A20^{fl/fl}$ mice with or without T-cell depletion and $A20^{fl/fl}$ mice with T-cell depletion ($n = 8$ mice/group). (C) Serum levels of indicated cytokines were measured by cytometric bead arrays 3 h after LPS injection. Data are shown as mean + SEM of four mice per experimental group. (A–C) Data are representative of three independent experiments. $^*p < 0.05$, ANOVA test.

contribute to death by leakage of the intestinal barrier and induction of bacterial sepsis. To prove whether the intestinal flora contributed to the enhanced mortality of LPS-stimulated CD11c-Cre $A20^{fl/fl}$ mice, animals were treated with an antibiotic cocktail, which eliminated intestinal bacteria from birth until the age of 9 weeks (Fig. 5A). In contrast to T-cell depletion, antibiotic treatment did not reduce liver pathology, and had no influence on hepatic DC numbers and serum cytokine profile of CD11c-Cre $A20^{fl/fl}$ mice (Supporting Information Fig. 7), which is consistent with the previous report that spontaneous activation of A20-deficient DCs is regulated by MyD88-independent signals [17]. Upon LPS stimulation, antibiotic treatment did not prevent death of CD11c-Cre $A20^{fl/fl}$ mice but only slightly prolonged the survival (Fig. 5B). The slightly but not significantly delayed death of CD11c-Cre $A20^{fl/fl}$ mice was reflected by partially reduced serum levels of IL-2, IL-12, IFN-γ, and IL-10 (Fig. 5C).

A20-deficient DCs are responsible for low-dose LPS induced mortality of CD11c-Cre $A20^{fl/fl}$ mice

To further study the role of DCs and their A20 expression in LPS tolerance, we transferred equal amounts of A20-deficient and A20-sufficient FLT3L-expanded BMDCs, respectively, to $A20^{fl/fl}$ control mice. Low-dose LPS induced mortality only in recipients of A20-deficient FLT3L-expanded BMDCs but not in recipients of A20-sufficient FLT3L-expanded BMDCs and mice without BMDC transfer (Fig. 6A). In contrast to FLT3L-expanded BMDCs, the more proinflammatory GM-CSF-expanded BMDCs induced mortality in recipients of both A20-sufficient and A20-deficient BMDCs (Fig. 6B). However, recipients receiving A20-deficient GM-CSF-expanded BMDCs died earlier and significantly more than mice supplemented with A20-sufficient GM-CSF-expanded BMDCs (Fig. 6B). The increased mortality in mice receiving GM-CSF-expanded BMDCs was paralleled by increased serum levels of cytokines (Fig. 6C). Thus irrespective of FLT3L- or GM-CSF-mediated polarization and expansion of BMDCs, increase and presence of A20-deficient BMDCs renders A20 sufficient mice susceptible to low-dose LPS challenge.

Discussion

In addition to their important roles in immunity, DCs are the key regulators of immune homeostasis under steady-state conditions. The present study demonstrates a pivotal role of DC-specific A20 in inhibiting the activation of DCs and protecting mice from developing spontaneous multi-organ inflammation (Supporting Information Fig. 1), which is consistent with previous reports [17, 18]. However, we show that CD11c-Cre $A20^{fl/fl}$ mice developed spontaneous hepatitis, which was not observed in previous reports [17, 18]. Of note, two other independent mouse strains with DC-specific A20 ablation also differed in their disease phenotype, showing that the clinical manifestations of A20-deficiency in DCs are variable. It has been suggested that the divergent luminal microbiota contribute to the phenotypic differences [14, 24]. In addition, subtle genetic differences between the mouse strains might also account for the different disease spectrum [24]. In extension of a previous report that demonstrated that the spontaneous inflammatory disease in mice with A20-deficient DCs

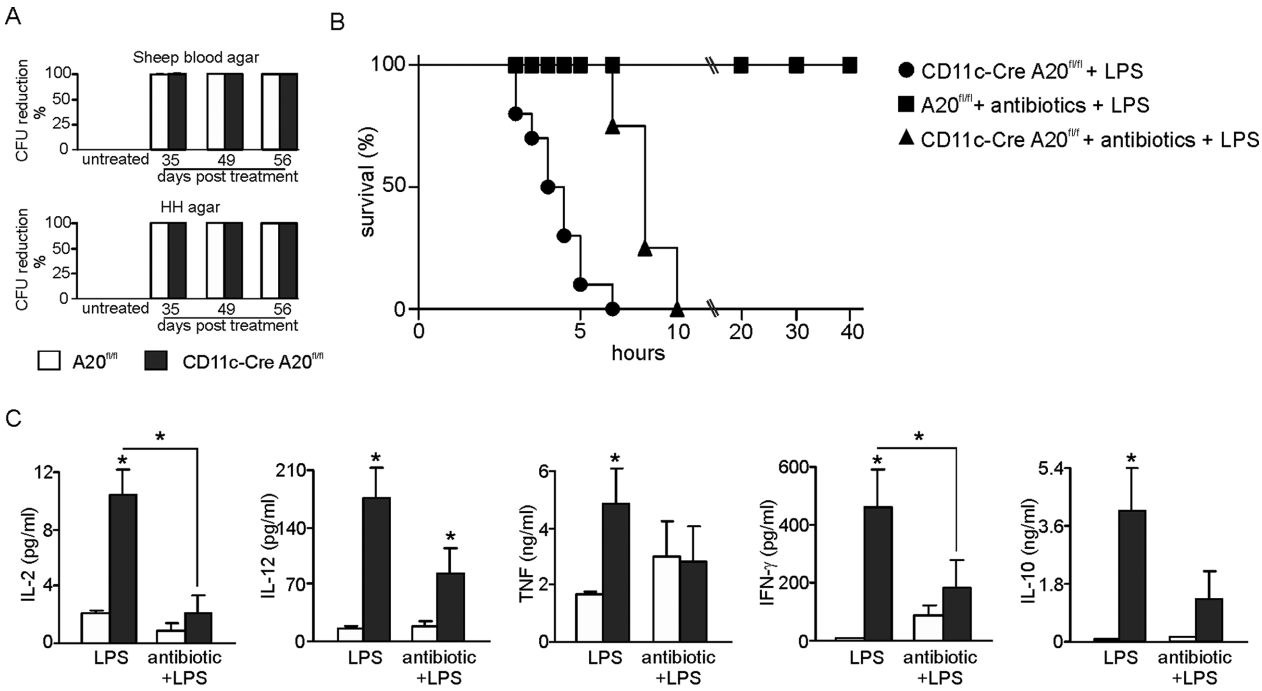

Figure 5. Intestinal bacteria depletion does not rescue CD11c-Cre A20$^{fl/fl}$ mice from sublethal dose of LPS-mediated mortality. (A) Reduction of colony forming units in stool samples of untreated and antibiotics-treated A20$^{fl/fl}$ and CD11c-Cre A20$^{fl/fl}$ mice was determined with sheep blood agar (upper panel) and HH agar (lower panel), respectively. Data are shown as mean + SEM of five mice per experimental group. (B) Survival of LPS-treated CD11c-Cre A20$^{fl/fl}$ mice with or without antibiotic treatment and LPS plus antibiotic-treated A20$^{fl/fl}$ mice ($n = 6$ mice/experimental group). (C) Serum levels of indicated cytokines were measured by cytometric bead arrays 3 h after LPS injection. Data show the mean + SEM of five mice per experimental group. (A–C) Data are from one experiment representative of three independent experiments. $^*p < 0.05$, ANOVA test.

was independent of MyD88 signaling [17], we also observed that the elimination of intestinal bacteria did not prevent multiorgan inflammation in CD11c-Cre A20$^{fl/fl}$ mice. Thus, the activation of A20-deficient DCs and the resulting chronic inflammatory disease is independent of bacteria-driven PAMP/TLR-MyD88 pathways.

Importantly and in sharp contrast, stimulation of TLR4 by low-dose LPS treatment induced rapid mortality in CD11c-Cre A20$^{fl/fl}$ mice. Within 3 h after LPS challenge, both proinflammatory and anti-inflammatory cytokines were significantly elevated in serum of CD11c-Cre A20$^{fl/fl}$ mice as compared with the control mice, showing that CD11c-Cre A20$^{fl/fl}$ mice suffered from uncontrolled cytokine production that resulted from both increased DC numbers and DC cytokine production. Consequently, CD11c-Cre A20$^{fl/fl}$ mice died within 6 h, whereas control mice survived.

Consistent with an inhibitory function of A20 in NF-κB signaling, LPS-mediated activation of NF-κB was enhanced in the absence of A20 explaining the increased cytokine production of A20-deficient DCs. Interestingly, IL-2 production was also significantly elevated in LPS-stimulated A20-deficient DCs. In addition to NF-κB, AP-1, and NFAT also contribute to IL-2 production [25]. Among NFAT members, NFATc3 is especially important for the induction of IL-2 [26]. Upon stimulation, NFATc3 is dephosphorylated following calmodulin-calcineurin activation and translocates to the nucleus to start gene transcription. In addition to the calcineurin pathway [27, 28], ERK activity is also required for IL-2 production in DCs [29]. Here, we additionally found that activation of the TAK1-MEK1-ERK1/2 signaling cascade was strongly upregulated in A20-deficient DCs after LPS stimulation and contributed to NFATc3 translocation and IL-2 production. Importantly, the ERK1/2 inhibition abolished the increased nuclear accumulation of NFATc3 and the increased IL-2 production in A20-deficient DCs. In contrast, calcineurin expression was equal in A20-deficient and A20-sufficient DCs (data not shown), indicating that the calcineurin pathway was not critically regulated by A20. Taken together, these results show that A20 suppressed ERK1/2-dependent NFAT activation in DCs, thereby inhibiting IL-2 production.

Given that LPS-stimulated T cells are an important source of Th1 cytokines, it is possible that the mortality of these animals was caused by hyperactivated T cells. However, T-cell depletion only slightly delayed the death of LPS-challenged CD11c-Cre A20$^{fl/fl}$ mice showing that T cells did not contribute vitally to their enhanced sensitivity to LPS. In addition, T-cell-depleted A20$^{fl/fl}$ control mice lost body weight, failed to recover and succumbed in response to low dose of LPS indicating that T cells are beneficial, instead of detrimental, during LPS stimulation. With respect to the multiorgan inflammation of non-LPS challenged CD11c-Cre A20$^{fl/fl}$ mice, T-cell depletion slightly ameliorated liver pathology indicating that this spontaneous disease was partially mediated by T cells.

Since (i) mice with deficient A20 expression in DCs develop spontaneous multiorgan inflammation ([17, 18], this study),

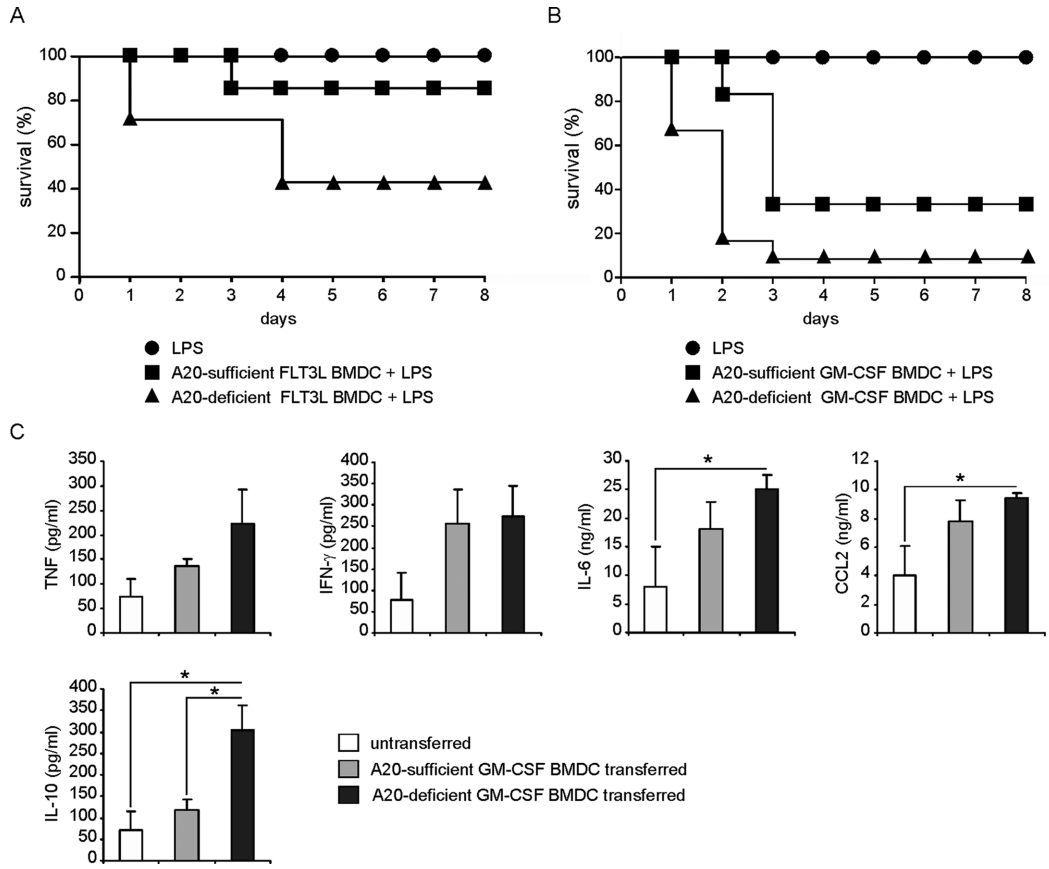

Figure 6. A20-deficient dendritic cells sensitize mice to LPS-mediated mortality. (A) Survival of $A20^{fl/fl}$ mice, $A20^{fl/fl}$ mice receiving A20-sufficient FLT3L BMDCs, and $A20^{fl/fl}$ mice receiving A20-deficient FLT3L BMDCs after LPS challenge. Data are pooled from two independent experiments, with a total of 7–10 mice per experimental group. Significant differences were found between A20-sufficient and A20-deficient FLT3L BMDCs transferred groups (log-rank test; $p < 0.05$). (B) Survival of $A20^{fl/fl}$ mice, $A20^{fl/fl}$ mice receiving A20-sufficient GM-CSF BMDCs, and $A20^{fl/fl}$ mice receiving A20-deficient GM-CSF BMDCs after LPS challenge. Data are pooled from two independent experiments, with a total of 8–12 mice per experimental group. Significant differences were found between A20-sufficient and A20-deficient GM-CSF BMDCs transferred groups (log-rank test; $p < 0.05$). (C) Serum levels of cytokines and chemokines of GM-CSF BMDCs transferred mice were measured by cytometric bead arrays 16 h after LPS injection. Data are shown as mean + SEM of 4–5 mice per experimental group, and are from one experiment representative of two independent experiments. $^*p < 0.05$, ANOVA test.

(ii) LPS strongly activates A20-deficient DCs (Fig. 2), and (iii) intestinal bacteria are a constant source of low doses of LPS stimulating the immune system [30], we studied the functional role of the intestinal flora on both the spontaneous induction of inflammation as well as mortality induced by LPS challenge. Depletion of the intestinal flora by antibiotic treatment from birth until 9 weeks did neither affect the onset of inflammation in non-LPS challenged nor the mortality of LPS-challenged CD11c-Cre $A20^{fl/fl}$ mice. Thus, the intestinal flora is not a critical regulator of A20-dependent LPS tolerance under normal and exogenous LPS-induced pathophysiological conditions.

In both humans and mice, DCs undergo apoptosis during sepsis [31, 32]. This might be a protective mechanism that prevents the hosts from lethal overshooting immune responses, although the following immune suppression predisposes the host to secondary infections [33, 34]. However, depletion of $CD11c^+$ DCs before onset of sepsis renders mice more sensitive to polymicrobial sepsis [35] indicating that both the number and function of DCs have to be tightly balanced to combat sepsis. Consistently, we also observed that immunocompetent mice having received additional A20-sufficient GM-CSF-expanded BMDCs were more sensitive to LPS showing that an excess of proinflammatory DCs is detrimental during LPS challenge and prevents tolerance to LPS. Of note, increased mortality of A20-competent recipient mice was observed after transfer of both A20-deficient FLT3L- and GM-CSF-expanded BMDCs, whereas only A20-sufficient GM-CSF- but not FLT3L-expanded BMDCs induced mortality in low-dose LPS-challenged mice. These data illustrate that, not the total numbers of DCs but their polarization status as well as their A20-regulated sensitivity to LPS determines their negative role in survival upon LPS challenge. However, the difference in mortality and cytokine levels between recipients of A20-deficient and A20-sufficient BMDCs were not as dramatic as that between CD11c-Cre $A20^{fl/fl}$ and $A20^{fl/fl}$ mice. One reason underlying these data is that CD11c-Cre $A20^{fl/fl}$ mice had nearly threefold more DCs than $A20^{fl/fl}$ mice whereas in the adoptive DC transfer experiments mice received equal numbers of DCs. These results strongly indicate that LPS-induced mortality of CD11c-Cre $A20^{fl/fl}$ mice is synergistically

caused both by the quantitative increase and a hyperactivation of A20-deficient DCs. In conclusion, the present study discloses that DC-specific A20 is not only crucial to maintain immune homeostasis under steady-state conditions but also critically involved in LPS tolerance.

Materials and methods

Mice

Specific pathogen-free C57BL/6 $A20^{fl/fl}$ [36] mice were crossed with CD11c-Cre mice [37] to obtain CD11c-Cre $A20^{fl/fl}$ and $A20^{fl/fl}$ control mice. Genotyping of offsprings was carried out by PCR of tail DNA with primers targeting CD11c-Cre, and $A20^{fl/fl}$ respectively. Animal care and experimental procedures were performed according to the German animal protection law and approved by state authorities (Landesverwaltungsamt Halle, Germany; reference number 42502-2-994).

Blood tests

Serum levels of chemokine (C-C motif) ligand 2 (CCL2), IL-2, IL-6, IL-10, IL-12, IFN-γ, TNF, FLT3L were determined with Murine Cytometric Bead Arrays (BD, Heidelberg, Germany) according to manufacturer' instructions. Serum alanine aminotransferase and aspartate aminotransferase were measured on the Cobas Modular platform (Roche, Mannheim, Germany).

Bone marrow-derived DCs

Bone marrow-derived DCs were obtained and cultivated as described before [38, 39]. Cultures were supplemented with GM-CSF (35 ng/mL, Peprotech Tebu-bio, Offenbach, Germany) or FLT3L (200 ng/mL, Peprotech Tebu-bio, Offenbach, Germany) and fed with fresh GM-CSF or FLT3L containing medium on days 3 and 6, respectively. Nonadherent and loosely adherent cells were harvested after 8 days of culture. At day 8, >80% of the cells were $CD11c^+$. GM-CSF BMDCs (3.3×10^5/mL) were treated with LPS (0.5 μg/mL, *Escherichia coli* serotype 055:B5; Sigma) for indicated time points.

Flow cytometry

Hepatic and splenic leukocytes were isolated as described before [40]. Cells were stained with fluorochrome-coupled antibodies to CD45, CD3, CD8α, CD11c, DC-SIGN, PDCA-1, CD40, MHC II, CD11b, CD103, and CD86 as indicated. For intracellular cytokine staining of IL-2, IL-12, and TNF, cells were incubated with brefeldin A (10 μg/mL, Sigma) for 4 h. Flow cytometry was performed on a FACSCanto II (BD).

Western blotting

Cultured BMDCs were stimulated as indicated and lysed in RIPA1 buffer. Cytoplasmic and nuclear protein was isolated with NE-PER Nuclear and Cytoplasmic Extraction Kit (Thermo Scientific). Lysates were centrifuged at 14 000g for 20 min at 4°C. Supernatants were harvested and heated in lane marker reducing sample buffer (Thermo Scientific) for 5 min. WB was performed with antibodies specific for A20 (Imgenex, San Diego, CA), GAPDH, p38, p-p38, TAK1, p-TAK1, ERK1/2, p-ERK1/2, MEK1, p-MEK1 (all from Cell Signaling, Danvers, MA), IκB-α, p-IκB-α, c-Jun, p-c-Jun, NFATc3, β-tubulin, and histone deacetylase 1 (all from Santa Cruz Biotechnology, Dallas, USA). WB images were obtained with an INTAS image analysis system (INTAS, Göttingen, Germany) and results were analyzed with LabImage 1D software (Kapelan Bio-Imaging Solutions, Leipzig, Germany).

In vivo *LPS treatment*

LPS (*Escherichia coli* serotype 055:B5; Sigma) was i.p. injected in mice at 10 mg/kg body weight. Survival was monitored every 30 min within the first 10 h and every 12 h afterwards for 11 days.

In vivo T-cell depletion

Mice were i.p. treated with rat anti-mouse CD4 (clone GK1.5) plus anti-CD8 (clone 2.43; 0.5 mg each per mouse) and rat IgG (Sigma, 1 mg per mouse), respectively, at days 21, 22, 23, 27, 30, 33, 37, 51, 55 after birth. Efficiency of T-cell depletion was determined by flow cytometry.

Antibiotic treatment

The drinking water of mice was supplemented with polymyxin B (0.2 mg/mL), neomycin (0.4 mg/mL), rifaximin (0.1 mg/mL, all from Sigma), ampicillin (0.5 mg/mL; Ratiopharm, Ulm, Germany), and vancomycin (0.25 mg/mL; Hikma, Gräfeling, Germany) for 9 weeks starting at birth. The drinking water was changed every 12 h. The reduction of CFU per mg feces was calculated for antibiotic versus PBS-treated mice by plating fecal samples, dissolved in 1 mL sterile PBS, on Brain Heart Infusion and sheep blood agar plates, and counting CFU after 48 h.

BMDC transfer

Two million BMDCs in 200 μL PBS were i.v. injected into each mouse. Three hours later, mice were i.p. injected with 10 mg/kg LPS. Survival was monitored everyday for 8 days.

Histology

Liver, spleen, heart, lung, kidney, and colon were prepared as described [41]. Paraffin sections were stained with H&E and periodic acid Schiff reaction, respectively.

Statistics

Data are provided as means ± SEM. All experiments were performed at least two times. Statistical significance was determined using Student's unpaired two-tailed *t*-test or for multiple group analysis by one-way ANOVA with post Mann–Whitney U test with GraphPad Prism5 software. Statistical differences between survival curves were determined using Log-rank test with GraphPad Prism5 software. For all statistical analysis, p values < 0.05 were accepted as significant.

Acknowledgments: This work was supported by a grant of the Deutsche Forschungsgemeinschaft to D.S. and M.N. (SFB 845, TP5). The excellent technical assistance of Elena Fischer, Nadja Schlüter, and Annette Sohnekind is gratefully acknowledged.

Conflict of interest: The authors declare no financial or commercial conflict of interest.

References

1 **Steinman, R. M. and Banchereau, J.**, Taking dendritic cells into medicine. *Nature* 2007. **449**: 419–426.

2 **Reis e Sousa**, Dendritic cells in a mature age. *Nat. Rev. Immunol.* 2006. **6**: 476–483.

3 **Iwasaki, A. and Medzhitov, R.**, Toll-like receptor control of the adaptive immune responses. *Nat. Immunol.* 2004. **5**: 987–995.

4 **Kawai, T. and Akira, S.**, The roles of TLRs, RLRs and NLRs in pathogen recognition. *Int. Immunol.* 2009. **21**: 317–337.

5 **O'Neill, L. A., Golenbock, D. and Bowie, A. G.**, The history of Toll-like receptors - redefining innate immunity. *Nat. Rev. Immunol.* 2013. **13**: 453–460.

6 **Yamamoto, M., Sato, S., Hemmi, H., Hoshino, K., Kaisho, T., Sanjo, H., Takeuchi, O. et al.**, Role of adaptor TRIF in the MyD88-independent toll-like receptor signalling pathway. *Science* 2003. **301**: 640–643.

7 **Kagan, J. C. and Medzhitov, R.**, Phosphoinositide-mediated adaptor recruitment controls Toll-like receptor signalling. *Cell* 2006. **125**: 943–955.

8 **Zanoni, I., Ostuni, R., Marek, L. R., Barresi, S., Barbalat, R., Barton, G. M., Granucci, F. and Kagan, J. C.**, CD14 controls the LPS-induced endocytosis of Toll-like receptor 4. *Cell* 2011. **147**: 868–880.

9 **Ostuni, R., Zanoni, I., and Granucci, F.**, Deciphering the complexity of Toll-like receptor signalling. *Cell Mol. Life Sci.* 2010. **67**: 4109–4134.

10 **Fitzgerald, K. A., Rowe, D. C., Barnes, B. J., Caffrey, D. R., Visintin, A., Latz, E., Monks, B. et al.**, LPS-TLR4 signalling to IRF-3/7 and NF-kappaB involves the toll adapters TRAM and TRIF. *J. Exp. Med.* 2003. **198**: 1043–1055.

11 **Kagan, J. C., Su, T., Horng, T., Chow, A., Akira, S. and Medzhitov, R.**, TRAM couples endocytosis of Toll-like receptor 4 to the induction of interferon-beta. *Nat. Immunol.* 2008. **9**: 361–368.

12 **Hymowitz, S. G. and Wertz, I. E.**, A20: from ubiquitin editing to tumour suppression. *Nat. Rev. Cancer* 2010. **10**: 332–341.

13 **Wertz, I. E., O'Rourke, K. M., Zhou, H., Eby, M., Aravind, L., Seshagiri, S., Wu, P. et al.**, De-ubiquitination and ubiquitin ligase domains of A20 downregulate NF-kappaB signalling. *Nature* 2004. **430**: 694–699.

14 **Ma, A. and Malynn, B. A.**, A20: linking a complex regulator of ubiquitylation to immunity and human disease. *Nat. Rev. Immunol. 2012.* **12**: 774–785.

15 **Shembade, N., Ma, A. and Harhaj, E. W.**, Inhibition of NF-kappaB signalling by A20 through disruption of ubiquitin enzyme complexes. *Science* 2010. **327**: 1135–1139.

16 **Lee, E. G., Boone, D. L., Chai, S., Libby, S. L., Chien, M., Lodolce, J. P. and Ma, A.**, Failure to regulate TNF-induced NF-kappaB and cell death responses in A20-deficient mice. *Science* 2000. **289**: 2350–2354.

17 **Hammer, G. E., Turer, E. E., Taylor, K. E., Fang, C. J., Advincula, R., Oshima, S., Barrera, J. et al.**, Expression of A20 by dendritic cells preserves immune homeostasis and prevents colitis and spondyloarthritis. *Nat. Immunol. 2011.* **12**: 1184–1193.

18 **Kool, M., van, L. G., Waelput, W., De, P. S., Muskens, F., Sze, M., van, P. J. et al.**, The ubiquitin-editing protein A20 prevents dendritic cell activation, recognition of apoptotic cells, and systemic autoimmunity. *Immunity* 2011. **35**: 82–96.

19 **Turer, E. E., Tavares, R. M., Mortier, E., Hitotsumatsu, O., Advincula, R., Lee, B., Shifrin, N. et al.**, Homeostatic MyD88-dependent signals cause lethal inflamMation in the absence of A20. *J. Exp. Med. 2008.* **205**: 451–464.

20 **Maraskovsky, E., Pulendran, B., Brasel, K., Teepe, M., Roux, E. R., Shortman, K., Lyman, S. D. and McKenna, H. J.**, Dramatic numerical increase of functionally mature dendritic cells in FLT3 ligand-treated mice. *Adv. Exp. Med. Biol. 1997.* **417**: 33–40.

21 **Zanoni, I., Ostuni, R., Capuano, G., Collini, M., Caccia, M., Ronchi, A. E., Rocchetti, M. et al.**, CD14 regulates the dendritic cell life cycle after LPS exposure through NFAT activation. *Nature* 2009. **460**: 264–268.

22 **Kim, K. D., Zhao, J., Auh, S., Yang, X., Du, P., Tang, H. and Fu, Y. X.**, Adaptive immune cells temper initial innate responses. *Nat. Med. 2007.* **13**: 1248–1252.

23 **Zhao, J., Kim, K. D., Yang, X., Auh, S., Fu, Y. X. and Tang, H.**, Hyper innate responses in neonates lead to increased morbidity and mortality after infection. *Proc. Natl. Acad. Sci. USA* 2008. **105**: 7528–7533.

24 **Hammer, G. E. and Ma, A.**, Molecular control of steady-state dendritic cell maturation and immune homeostasis. *Annu. Rev. Immunol.* 2013. **31**: 743–791.

25 **Granelli-Piperno, A. and Nolan, P.**, Nuclear transcription factors that bind to elements of the IL-2 promoter. *Induction requirements in primary human T cells. J. Immunol.* 1991. **147**: 2734–2739.

26 **Urso, K., Alfranca, A., Martinez-Martinez, S., Escolano, A., Ortega, I., Rodriguez, A. and Redondo, J. M.**, NFATc3 regulates the transcription of genes involved in T-cell activation and angiogenesis. *Blood* 2011. **118**: 795–803.

27 **Goodridge, H. S., Simmons, R. M. and Underhill, D. M.**, Dectin-1 stimulation by *Candida albicans* yeast or zymosan triggers NFAT activation in macrophages and dendritic cells. *J. Immunol.* 2007. **178**: 3107–3115.

28 **O'Keefe, S. J.**, **Tamura, J.**, **Kincaid, R. L.**, **Tocci, M. J. and O'Neill, E. A.**, FK-506- and CsA-sensitive activation of the interleukin-2 promoter by calcineurin. *Nature* 1992. **357**: 692–694.

29 **Slack, E. C.**, **Robinson, M. J.**, **Hernanz-Falcon, P.**, **Brown, G. D.**, **Williams, D. L.**, **Schweighoffer, E.**, **Tybulewicz, V. L. and Reis e Sousa**, Syk-dependent ERK activation regulates IL-2 and IL-10 production by DC stimulated with zymosan. *Eur. J. Immunol.* 2007. **37**: 1600–1612.

30 **Goto, Y. and Kiyono, H.**, Epithelial barrier: an interface for the cross-communication between gut flora and immune system. *Immunol. Rev.* 2012. **245**: 147–163.

31 **Tinsley, K. W.**, **Grayson, M. H.**, **Swanson, P. E.**, **Drewry, A. M.**, **Chang, K. C.**, **Karl, I. E. and Hotchkiss, R. S.**, Sepsis induces apoptosis and profound depletion of splenic interdigitating and follicular dendritic cells. *J. Immunol.* 2003. **171**: 909–914.

32 **Hotchkiss, R. S.**, **Tinsley, K. W.**, **Swanson, P. E.**, **Grayson, M. H.**, **Osborne, D. F.**, **Wagner, T. H.**, **Cobb, J. P. et al.**, Depletion of dendritic cells, but not macrophages, in patients with sepsis. *J. Immunol.* 2002. **168**: 2493–2500.

33 **Benjamim, C. F.**, **Lundy, S. K.**, **Lukacs, N. W.**, **Hogaboam, C. M. and Kunkel, S. L.**, Reversal of long-term sepsis-induced immunosuppression by dendritic cells. *Blood* 2005. **105**: 3588–3595.

34 **Benjamim, C. F.**, **Hogaboam, C. M. and Kunkel, S. L.**, The chronic consequences of severe sepsis. *J. Leukoc. Biol.* 2004. **75**: 408–412.

35 **Scumpia, P. O.**, **McAuliffe, P. F.**, **O'Malley, K. A.**, **Ungaro, R.**, **Uchida, T.**, **Matsumoto, T.**, **Remick, D. G. et al.**, CD11c+ dendritic cells are required for survival in murine polymicrobial sepsis. *J. Immunol.* 2005. **175**: 3282–3286.

36 **Wang, X.**, **Deckert, M.**, **Xuan, N. T.**, **Nishanth, G.**, **Just, S.**, **Waisman, A.**, **Naumann, M. and Schluter, D.**, Astrocytic A20 ameliorates experimental autoimmune encephalomyelitis by inhibiting NF-kappaB- and STAT1-dependent chemokine production in astrocytes. *Acta Neuropathol.* 2013. **126**: 711–724

37 **Caton, M. L.**, **Smith-Raska, M. R. and Reizis, B.**, Notch-RBP-J signalling controls the homeostasis of CD8- dendritic cells in the spleen. *J. Exp. Med.* 2007. **204**: 1653–1664.

38 **Xuan, N. T.**, **Shumilina, E.**, **Kempe, D. S.**, **Gulbins, E. and Lang, F.**, Sphingomyelinase dependent apoptosis of dendritic cells following treatment with amyloid peptides. *J. Neuroimmunol.* 2010. **219**: 81–89.

39 **Inaba, K.**, **Inaba, M.**, **Romani, N.**, **Aya, H.**, **Deguchi, M.**, **Ikehara, S.**, **Muramatsu, S. and Steinman, R. M.**, Generation of large numbers of dendritic cells from mouse bone marrow cultures supplemented with granulocyte/macrophage colony-stimulating factor. *J. Exp. Med.* 1992. **176**: 1693–1702.

40 **Sakowicz-Burkiewicz, M.**, **Nishanth, G.**, **Helmuth, U.**, **Drogemuller, K.**, **Busch, D. H.**, **Utermohlen, O.**, **Naumann, M. et al.**, Protein kinase C-theta critically regulates the proliferation and survival of pathogen-specific T cells in murine listeriosis. *J. Immunol.* 2008. **180**: 5601–5612.

41 **Haroon, F.**, **Drogemuller, K.**, **Handel, U.**, **Brunn, A.**, **Reinhold, D.**, **Nishanth, G.**, **Mueller, W. et al.**, Gp130-dependent astrocytic survival is critical for the control of autoimmune central nervous system inflammation. *J. Immunol.* 2011. **186**: 6521–6531.

Abbreviations: **BMDC**: bone marrow-derived dendritic cell · **FLT3L**: fms-related tyrosine kinase 3 ligand · **PPR**: pattern recognition receptor · **TAK1**: transforming growth factor-β activated kinase-1 · **WB**: Western blot

Full correspondence: Prof. Dirk Schlüter, Institute of Medical Microbiology and Hospital Hygiene, Otto-von-Guericke University Magdeburg, 39120 Magdeburg, Leipziger Str. 44, Germany
Fax: +49-0391-67290717
e-mail: dirk.schlueter@med.ovgu.de

Current address: Nguyen Thi Xuan, Institute of Genome Research, Vietnam Academy of Science and Technology, No.18, Hoang Quoc Viet, Cau Giay, Hanoi, Vietnam.

Received: 30/4/2014
Revised: 22/10/2014
Accepted: 28/11/2014
Accepted article online: 4/12/2014

European Journal of Immunology

Supporting Information

for

DOI 10.1002/eji.201444795

Nguyen Thi Xuan, Xu Wang, Gopala Nishanth, Ari Waisman, Katrin Borucki, Berend Isermann, Michael Naumann, Martina Deckert and Dirk Schlüter

A20 expression in dendritic cells protects mice from LPS-induced mortality

Supporting Information Fig. 1

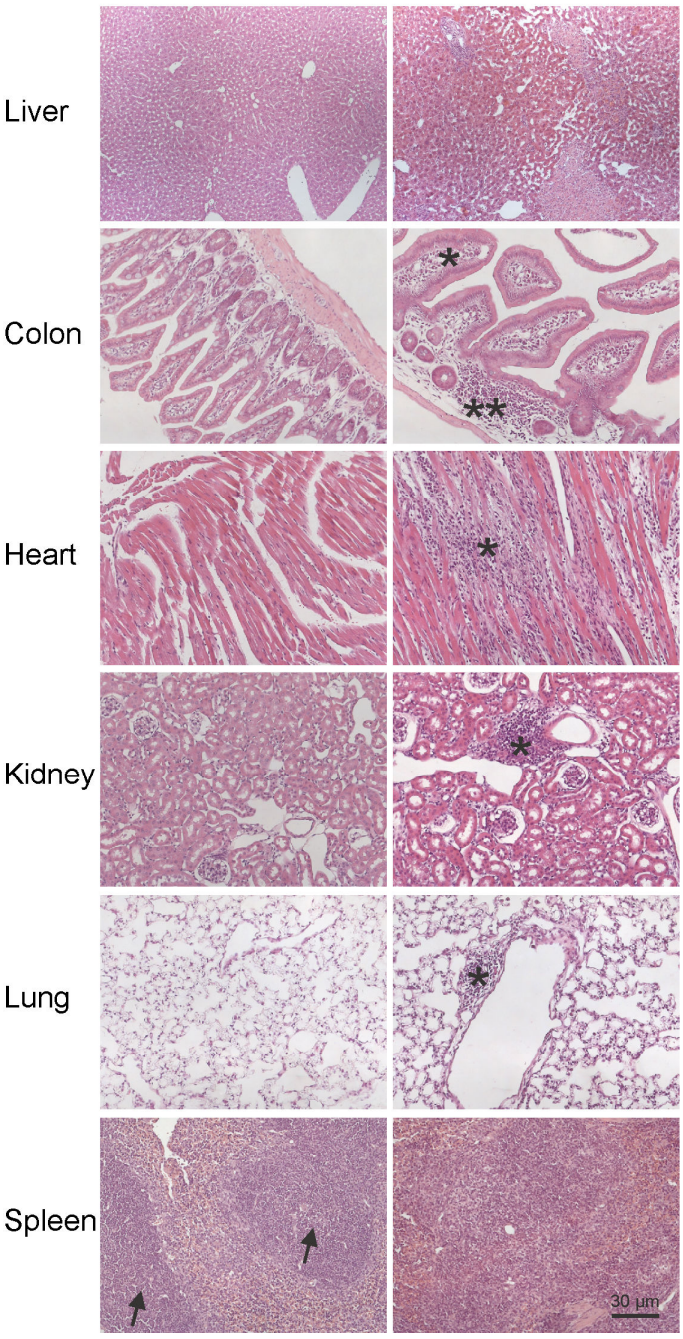

Supporting Information Fig. 1 Multi-organ inflammation in CD11c-Cre A20$^{fl/fl}$ mice (at the age of 12 months) involves liver, colon, heart, kidney, lung and spleen. Severe hepatitis affects both lobules and portal tracts; in the colon, the plump lamina propria harbors prominent inflammatory infiltrates (star); double star indicates a crypt abscess. In the myocardium, large inflammatory infiltrates have destroyed a group of myocytes (star). Mild glomerulonephritis with leukocytes clustering perivascularly (star). Peribronchiolar intraalveolar lymphocytic infiltrates as evidence of mild lung inflammation (star). The architecture of the spleen is disturbed. In contrast to WT mice (arrow), which harbors well-delineated follicles, the follicular structure is altered due to accumulation of large number of erythroblasts. H&E staining, original magnification × 200.

Supporting Information Fig. 2

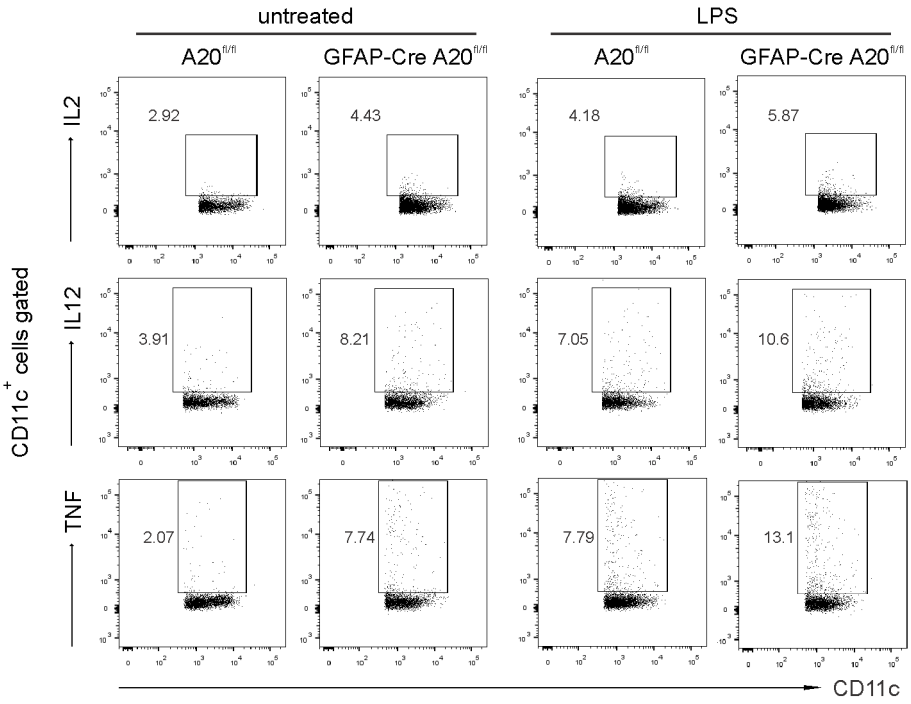

Supporting Information Fig. 2 Representative dot plots show the percentage of IL-2-, IL-12-, and TNF-producing DCs before and after LPS stimulation.

Supporting Information Fig. 3

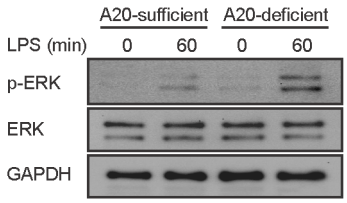

Supporting Information Fig. 3 WB analysis of p-ERK, ERK and GAPDH in MACS-isolated splenic $CD11c^+$ cells unstimulated or stimulated with LPS (0.5 μg/ml) for 1 h.

Supporting Information Fig. 4

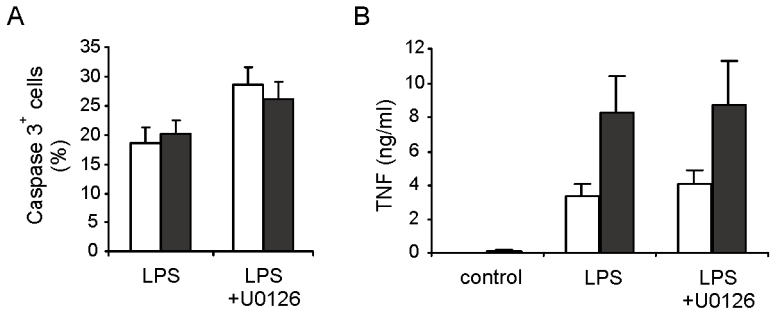

Supporting Information Fig. 4 Effect of ERK inhibition on cell apoptosis and TNF production. (A) GM-CSF BMDCs were treated with LPS (0.5 μg/ml) or LPS (0.5 μg/ml) plus U0126 (10 μM) and apoptotic cells were measured by Caspase 3 staining. (B) Concentrations of TNF produced by GM-CSF BMDCs untreated or treated with LPS (0.5 μg/ml) or LPS (0.5 μg/ml) plus U0126 (10 μM) for 24 hours were measured by CBA.

Supporting Information Fig. 5

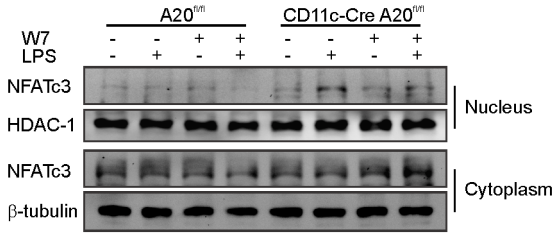

Supporting Information Fig. 5 WB analysis of cytoplasmic and nuclear extracts unstimulated or stimulated with LPS (0.5 μg/ml) and/or W7 (30 μM) for 1 hour.

Supporting Information Fig. 6

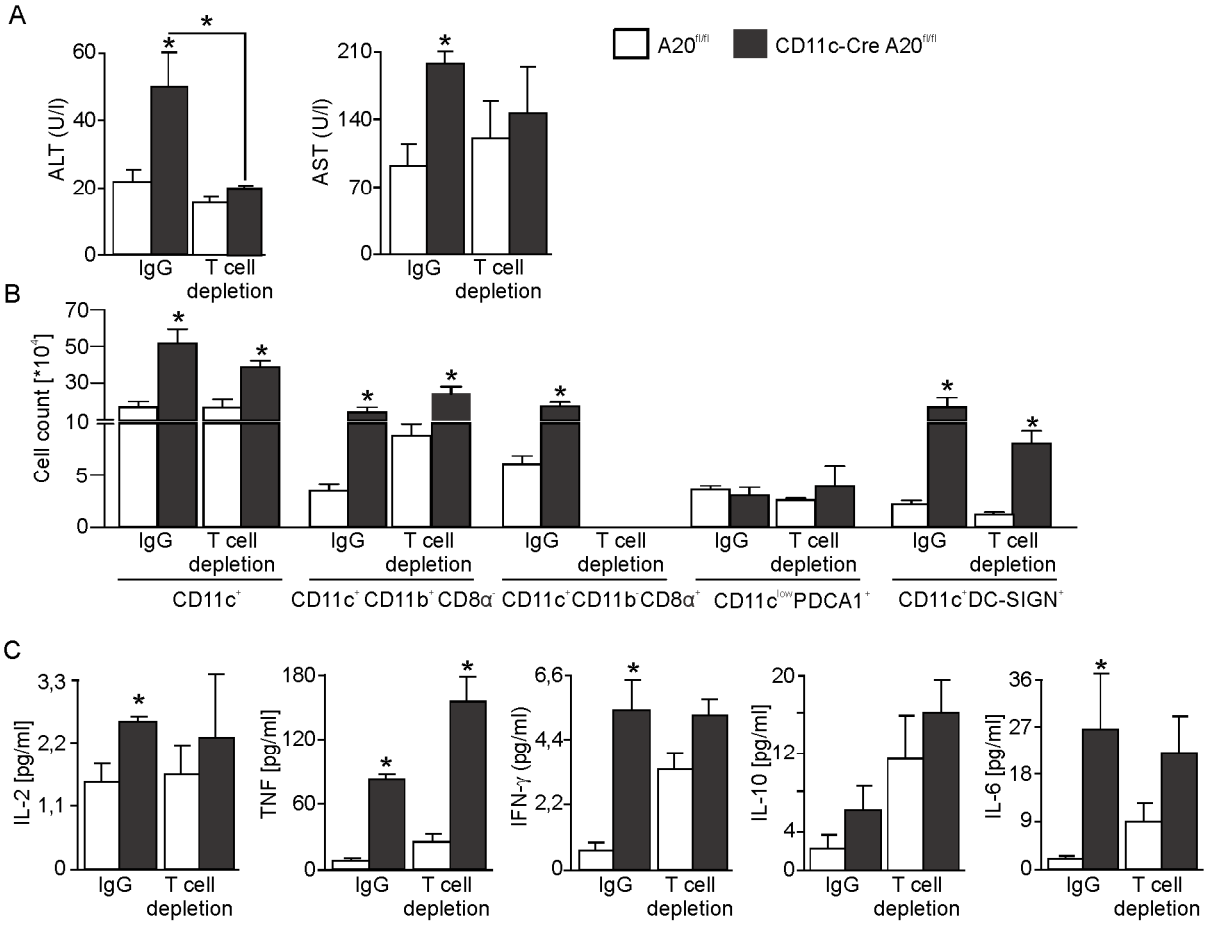

Supporting Information Fig. 6 Effect of T cell depletion on DCs and serum cytokine levels. (A) Levels of ALT and AST in serum (n = 5 per group, mean + SEM, *$P < 0.05$). (B) Numbers of total hepatic DCs and DC subpopulations were determined by flow cytometry (n = 5 per group, mean + SEM, *$P < 0.05$). (C) Serum cytokines were measured by CBA (n = 5 per group, mean + SEM, *$P < 0.05$).

Supporting Information Fig. 7

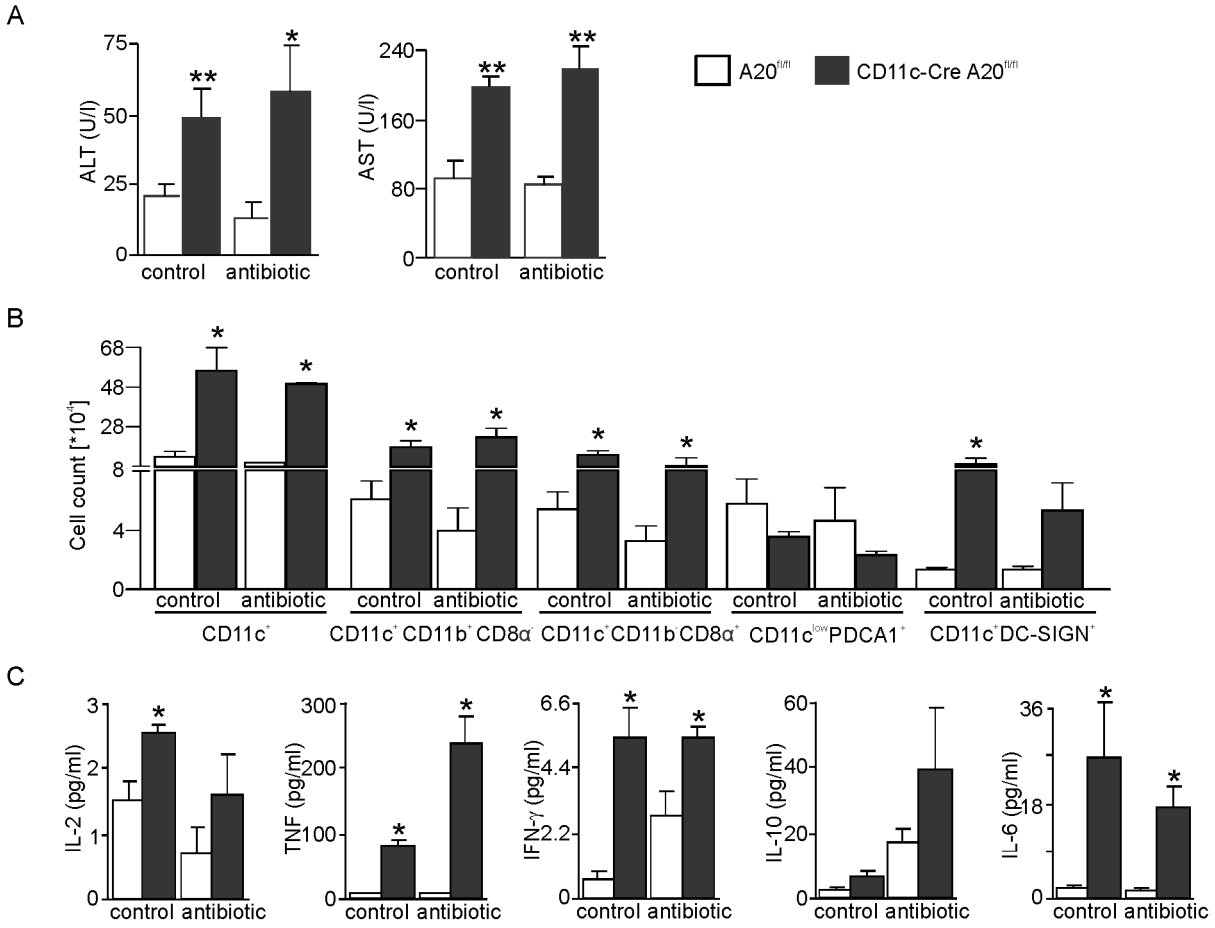

Supporting Information Fig. 7 Effect of antibiotic treatment on DCs and serum cytokine levels. (A) Levels of ALT and AST in serum (n = 5 per group, mean + SEM, $*P < 0.05$). (B) Numbers of total hepatic DCs and DC subpopulations of control (PBS) and antibiotic-treated $A20^{fl/fl}$ and CD11c-Cre $A20^{fl/fl}$ mice were determined by flow cytometry (n = 5 per group, mean + SEM, $*P < 0.05$). (C) Serum cytokines were measured by cytometric bead assay (n = 5 per group, mean + SEM, $*P < 0.05$).